High-speed infrared thermography for the measurement of microscopic boiling parameters on micro- and nano-structured surfaces

Youngjae Park [a], Hyungmo Kim [b], Joonwon Kim [c], Hyungdae Kim [a*]
[a] *Department of Nuclear Engineering, Kyung Hee Univ., Yongin, Korea*
[b] *Advanced Reactor Technology Development, KAERI, Daejeon, Korea*
[c] *Department of Mechanical Engineering, POSTECH, Pohang, Korea*
[*] *Corresponding author: hdkims@khu.ac.kr*

1. Introduction

Micro- and nano-scale structures on boiling surfaces can enhance nucleate boiling heat transfer coefficient (HTC) and critical heat flux (CHF) [1, 2, 3]. The improvements are closely related to changes in microscopic boiling parameters such as nucleation site density (N''), bubble departure frequency (f_d), and bubble departure diameter (D_d). A few studies were conducted to explain the enhancements of HTC and CHF using the microscopic boiling parameters. Mchale and Gerimella [4] reported that HTC was enhanced by increasing N'' and decreasing D_d and f_d on the rough surface. Theofanous et al. [5] studied the effects of N'' and radius of curvature of liquid meniscus underneath the boiling bubbles (related to D_d) to explain the enhancement of CHF on the aged surface.

Therefore, quantitative measurements of microscopic boiling parameters are needed to understand the physical mechanism of the boiling heat transfer augmentation on structured surfaces. However, there is no existing experimental techniques to conveniently measure the boiling parameters on the structured surfaces because of the small (<mm) and fast (~msec) scale of the physical phenomena.

In this study, we use a high-speed infrared (IR) thermography [6, 7] to visualize liquid-vapor phase distribution during nucleate pool boiling on micro- and nano-structured surfaces. The visualization results are analyzed to obtain the microscopic boiling parameters. Finally, quantitative microscopic boiling parameters are used to interpret the enhancement of HTC and CHF.

2. Experiments

2.1 Measurement principle

We use the IR thermography to visualize the phase distribution of liquid (water) and vapor (steam) on an IR transparent silicon heater. A combination of the IR transparent silicon heater and the IR opaque water were used in this study. This combination enables to visualize the liquid-vapor phase distributions on the boiling surface, because silicon has 55% transparency for 3-5 μm wavelength of infrared light. Detailed descriptions about the IR thermography for boiling experiments are described in previous works [6, 7] in detail.

There is no useful experimental technique to be able to visualize liquid-vapor phase distribution on micro- and nano-structured surfaces. We expect that in the IR thermography results, liquid-vapor phase distribution on structured surfaces would be visible thanks to the IR intensity difference between superheated liquid on the heater surface and relatively cold liquid beyond the boiling bubbles. Here we attempt to validate the IR thermography technique for the visualization of the two (liquid-vapor) phase distribution on micro- and nano-structures boiling surfaces.

2.2 Boiling experiments

Pool boiling apparatus was installed to conduct the boiling experiments. Immersion heater and reflux condenser were installed to maintain the saturation condition of pool at atmospheric pressure. IR camera was used to visualize the boiling phenomena above the heated surface through the installed high reflection (up to 98%) hot mirror underneath the silicon heater. The experimental procedure consisted of follows: assembling the apparatus with water, degassing it by pre-boiling the water for approximately two hours using immersion heater, and increase the applied heat flux in small steps with enough time (>1 min) to achieve the steady state.

Micro- and nano-structured surfaces were used for nucleate pool boiling experiments that were fabricated by photolithography (Fig. 1(a), M-surface) and black silicon method (Fig. 1(b), N-surface) as the MEMS techniques. Smooth surface note that the S-surface (Fig. 1(c)).

3. Results and discussions

3.1 visualization results

Figure 2 shows the boiling curves for the S-, M-, and N-surface. The HTC and CHF were enhanced on the structured surfaces. Most significant change of boiling phenomena is existed on the M-surface. ONB of M-surface was decreased 10 °C in comparison with 20 °C of S-surface. The HTC was increased with activation of bubble generation. The CHF of M- and N-surface were

also increased in comparison to S-surface. However, ONB and HTC of N-surface were not improved.

Fig. 3 shows the IR visualization results. In these visualization results, the dark area and bright area corresponds to boiling bubbles and superheated liquid, respectively. From the visualization image, liquid-vapor contact line was clearly distinguished as shown in Fig. 3.

The image of each surface is quite different. The M-surface has large number and small size of bubbles. However, S- and N-surface have relatively low number of bubbles, which is irregular shape. We expect that in the visualization results, the enhancement of HTC and CHF were analyzed by quantitative interpretation of liquid-vapor phase distributions, which are the microscopic boiling parameters.

3.2 Measurement of microscopic boiling parameters

The microscopic boiling parameters were analyzed by image processing as follows. Nucleation site density (N'') was picked the bubble nucleation site in image. Number density of dry patch (NDP) and Triple contact line density (TCLD) were measured by counting of dry patch and its perimeter through the threshold of IR intensities to distinguish liquid-vapor distributions.

Figures 4 and 5 show the N'' and TCLD of the tested surfaces. The N'' and TCLD was increased on the M-surface that led to enhance the HTC. Large number of the N'' [7] and TCLD [4, 8] lead to enhance the HTC. The present result corresponds to insight of HTC enhancement mechanism, as shown in Figs. 3 and 4.

Figures 6 and 7 show the NDP as a function of dry area size at 1000 kW/m^2 of heat flux and CHF, respectively. Just before the occurrence of CHF, as shown in Fig. 7, the number of large dry parch (> 5 mm) was increased in comparison with 1000 kW/m^2 of heat flux. This result supports the CHF model of modified hot/dry spot model [9].

The CHF enhancement was also explained by NDP. For the M- and N-surfaces, the number of large dry area was decreased in comparison with S-surface, because of the suppression of hot/dry spot formation.

The CHF enhancement of N-surface was probably affected by wettability and capillarity of the structures due to its hydrophilic characteristics [2]. The N-surface had 0° of static contact angle and large spreading area. However, this study was focused on the measurement of microscopic boiling parameters during nucleate boiling with structured surface. Hence, wettability and capillarity effects were not covered in detail.

4. Conclusions

In this study, liquid-vapor phase distributions of each surface were clearly visualized by IR thermography during the nucleate boiling phenomena. From the visualization results, following microscopic boiling parameters were quantitatively measured by image processing.

- Nucleation site density, N''
- Triple contact line density, TCLD
- Number density of dry patch, NDP

IR thermography technique was demonstrated by nucleate pool boiling experiments with M- and N-surfaces. The enhancement of HTC and CHF could be explained by microscopic boiling parameters.

Acknowledgement

This research was supported by Basic Science Research Program through the National Research Foundation of Korea (NRF) funded by the Ministry of Science, ICT & Future Planning (2012R1A1A1014779)

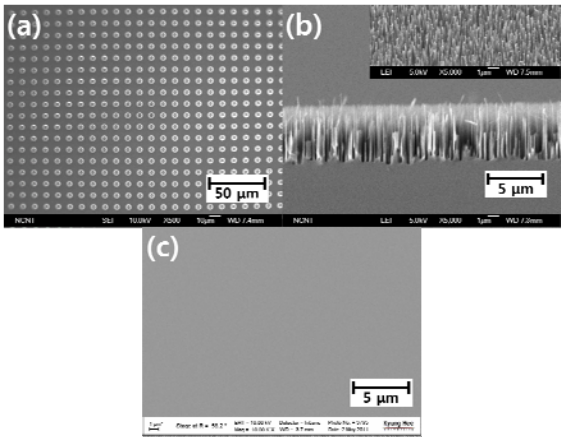

Fig. 1. SEM image of M-surface (a), N-surface (b), and S-surface (c).

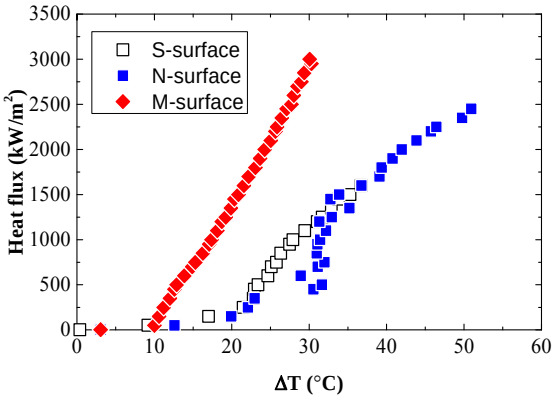

Fig. 2. Boiling curve of structured samples.

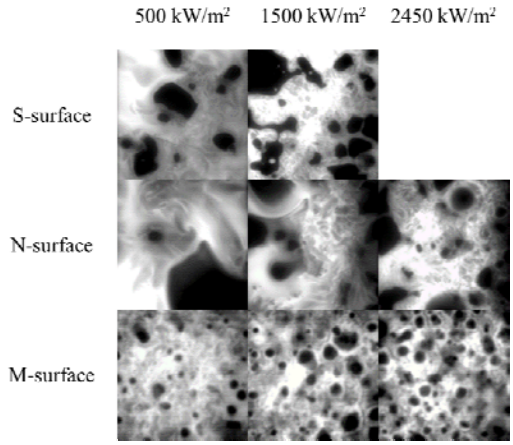

Fig. 3. Infrared snapshot of the various surfaces at increasing heat fluxes.

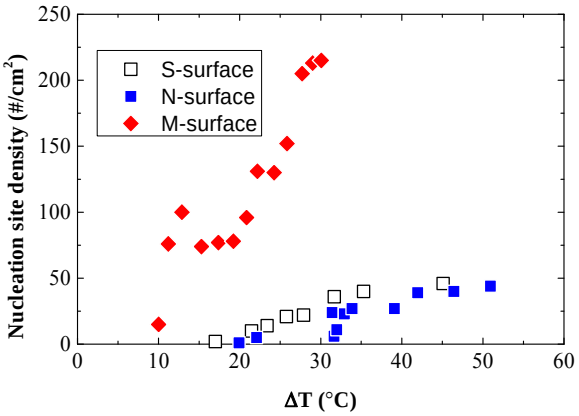

Fig. 4. Nucleation site density on the various samples as a function of wall superheat.

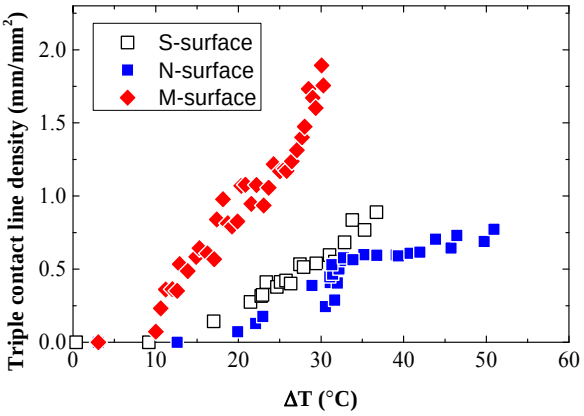

Fig. 5. Time-averaged triple (liquid-solid-vapor) contact line density on the various samples as a function of wall superheat.

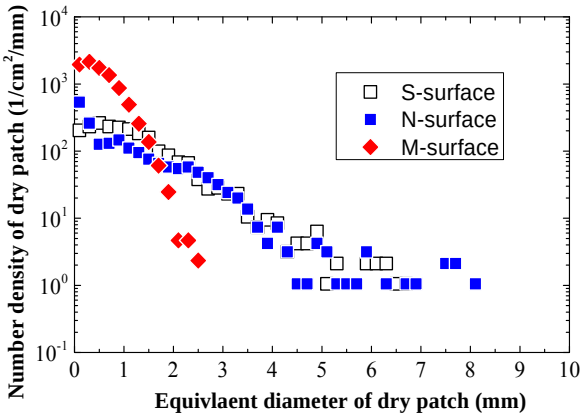

Fig. 6. Distribution of dry area number density depends on dry area diameter at 1000 kW/m².

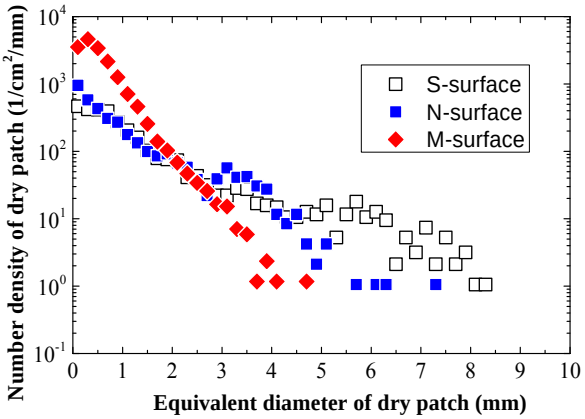

Fig. 7. Distribution of dry area number density depends on dry area diameter at CHF.

REFERENCES

[1] J. Wei, J. Zhao, M. Yuan, Y. Xue, Boiling heat transfer enhancement by using micro-pin-finned surface for electronics cooling, Microgravity Sci. Technol. vol. 21, Suppl. 1, pp. 159-173, 2009

[2] H.S. Ahn, C. Lee, H.D. Kim, H.J. Jo, S.H. Kang, J.W. Kim, J.S. Shin, M.H. Kim, Pool boiling CHF enhancement by micro/nanoscale modification of zircaloy-4 surface, Nuclear Engineering and Design, vol. 240, pp. 3350-3360, 2010

[3] R. Furberg, B. Palm, S. Li, M. Toprak, M. Muhammed, The use of a nano- and microporous surface layer to enhance boiling in a plate heat exchanger, Journal of Heat Transfer, vol. 131, 101010, 2009

[4] J.P. McHale, S.V. Garimella, Bubble nucleation characteristics in pool boiling of a wetting liquid on smooth and rough surfaces, International Journal of Multiphase Flow, vol. 36, pp. 249-260, 2010

[5] T.G. Theofanous, T.N. Dinh, J.P. Tu, A.T. Dinh, The boiling crisis phenomenon part II: dryout dynamics and burnout, Experimental Thermal and Fluid Science, vol. 26, pp. 793-810, 2002

[6] H.D. Kim, J. Buongiorno, Detection of liquid-vapor-solid triple contact line in two-phase heat transfer phenomena using high-speed infrared thermometry, International Journal of Multiphase Flow, vol. 37, pp. 166-172, 2011

[7] H.D. Kim, Y.J. Park, J. Buongiorno, Measurement of wetted area fraction in subcooled pool boiling of water using

infrared thermometry, Nuclear Engineering and Design, vol. 264, pp. 103-110, 2013
[8] R.J. Benjamin, A.R. Balakrishnan, Nucleation site density in pool boiling of saturated liquids: effect of surface microroughness and surface and liquid physical properties, Experimental thermal and fluid science, vol. 15, pp. 32-42, 1997
[9] I.C. Chu, Application of visualization techniques to the boiling structures of subcooled boiling flow and critical heat flux, Ph.D. Dissertation, KAIST, 2011